Proc. Natl. Acad. Sci. USA
Vol. 92, pp. 729–733, January 1995
Medical Sciences

Abnormal calcium homeostasis and mitochondrial polarization in a human encephalomyopathy

ANNA M. MOUDY*, SHAWN D. HANDRAN*, MARK P. GOLDBERG*, NATASHA RUFFIN*, IRENE KARL†, PAMELA KRANZ-EBLE‡, DARRYL C. DEVIVO‡, AND STEVEN M. ROTHMAN*§¶

*Center for the Study of Nervous System Injury, Department of Neurology, Box 8111, and †Division of Endocrinology and Metabolism, Department of Medicine, Box 8127, Washington University School of Medicine, St. Louis, MO 63110; ‡The Neurological Institute of New York, Columbia University College of Physicians and Surgeons, New York, NY 10032; and §Department of Neurology, St. Louis Children's Hospital, One Children's Place, St. Louis, MO 63110

Communicated by David M. Kipnis, Washington University, St. Louis, MO, October 3, 1994

ABSTRACT **Patients with several inherited human encephalomyopathies exhibit systemic and neurological symptoms in association with specific mitochondrial mutations. The mechanisms by which these mitochondrial mutations result in cellular injury have not been elucidated. One potential cause of neuronal vulnerability is an inability to effectively buffer intracellular calcium. We report that fibroblasts from patients with one specific inherited encephalomyopathy, MELAS (mitochondrial encephalomyopathy, lactic acidosis, and stroke-like episodes) syndrome, have elevated levels of ionized calcium and cannot normally sequester calcium influxes. Quantitative fluorescence imaging demonstrated that this abnormality was associated with a relative decrease in mitochondrial membrane potential compared to control fibroblasts. This documentation of pathological calcium homeostasis in a genetic neurological disease extends the calcium hypothesis of toxic cell injury to human mitochondrial encephalomyopathies.**

Several inherited human neurological diseases result from mitochondrial or nuclear genomic mutations that affect mitochondrial function (1–6). Impaired ATP production is an obvious candidate for the cellular dysfunction in these disorders, but we sought to determine a more specific link between mitochondrial defects and cellular injury. There is compelling evidence linking elevated intracellular Ca^{2+} (Ca_i^{2+}) to toxic cell damage (7–9). We examined Ca_i^{2+} and the mitochondrial energy state in cultured fibroblasts obtained from control patients and patients with MELAS (mitochondrial encephalomyopathy, lactic acidosis, and stroke-like episodes) syndrome (ref. 10; Table 1). This syndrome usually results from identifiable point mutations at nt 3243 or 3271 in the mitochondrial gene coding for a leucine tRNA (10–14). Patients with this disease exhibit posterior brain lesions, lactic acidosis, ragged red fibers, seizures, headache, vomiting, and dementia (2, 10–14). We anticipated that the disturbed cellular physiology responsible for these symptoms might be reflected in fibroblasts from affected patients.

MATERIALS AND METHODS

Cell Culture. Human fibroblasts were grown on glass coverslips and incubated in minimum essential medium (GIBCO) supplemented with 2 mM glutamine and 10% (vol/vol) NuSerum (Collaborative Research). Two to four sister dishes were used per passage and a minimum of two passages per patient were analyzed. No differences in calcium responses were noted between earlier and later passages. Mitochondrial DNA (mtDNA) analysis was done as described (10, 11). Analysis of fibroblast cultures in the MELAS group identified single point mutations at nt 3243 (patients M1–M3 in Table 1), nt 3271 (patient M4), and nt 8344 (patient M5, phenotypic for MELAS syndrome). The percentages of mutant mtDNA in these fibroblasts were as follows: M1, 71%; M2, not tested in fibroblasts but 64% in muscle; M3, 46%; M4, 67%; M5, 61% (10, 11). Southern blot analysis in the Kearns–Sayre (K–S) group identified no mtDNA deletion in patients K1 and K3 and 18% and 12% mutant mtDNA in patients K2 and K4, respectively (15).

ATP Analysis. ATP levels were assayed as described (16, 17).

Table 1. Ca_i^{2+} levels and mitochondrial polarization in MELAS and control fibroblasts

Patient	Age, years	Sex	Baseline Ca^{2+}, nM	% energized mitochondria
MELAS syndrome				
M1	0.6	M	164.6 ± 44.9	9.6 ± 11.9
M2	15.4	F	141.8 ± 35.6	10.2 ± 11.3
M3	19.3	M	127.4 ± 45.9	3.9 ± 5.6
M4	24	F	133.2 ± 49.7	10.5 ± 10.2
M5	16	M	149.4 ± 82.1	10.6 ± 8.8
Control				
C1	0	M	70.4 ± 7.2	45.8 ± 14.8
C2	0.75	F	76.6 ± 13.8	17.0 ± 9.2
C3	3.25	F	76.3 ± 24.5	19.1 ± 13.2
C4	20	M	77.3 ± 11.9	22.8 ± 16.4
C5	24	M	68.6 ± 7.1	24.9 ± 22.9
C6	25	F	96.4 ± 10.1	12.3 ± 11.4
C7	30	F	71.6 ± 13.3	22.3 ± 15.6
C8	45.4	F	92.0 ± 17.0	27.9 ± 18.0
C9	10.3	F	74.4 ± 20.0	16.8 ± 11.1
C10	Adult*	—	85.2 ± 19.3	17.0 ± 11.8
C11	Adult*	M	61.2 ± 25.8	NT
C12	Adult*	M	79.1 ± 19.2	11.9 ± 15.3
C13	Adult*	M	62.6 ± 14.7	NT
C14	0.08	F	71.9 ± 14.8	18.9 ± 9.5
K–S syndrome				
K1	10.5	M	83.8 ± 31.1	NT
K2	12.3	M	86.6 ± 36.9	NT
K3	15.8	M	85.7 ± 33.8	NT
K4	25	M	77.9 ± 27.9	NT

Percent energized mitochondria represents the fraction of mitochondrial pixels in which the ratio of the 590/527-nm JC-1 fluorescence is ≥1. Age and sex (M, male; F, female) were equally represented between control and MELAS groups. Within patient groups, no correlation was found between calcium values or mitochondrial potential and age or sex. Data are the mean ± SD. NT, not tested.
*Exact age at time of biopsy unknown.

The publication costs of this article were defrayed in part by page charge payment. This article must therefore be hereby marked "*advertisement*" in accordance with 18 U.S.C. §1734 solely to indicate this fact.

Abbreviations: MELAS, mitochondrial encephalomyopathy, lactic acidosis, and stroke-like episodes; Ca_i^{2+}, intracellular Ca^{2+}; K–S, Kearns–Sayre; PMT, photomultiplier tube.

¶To whom reprint requests should be sent at the § address.

Calcium Imaging. Cultures were incubated for 45 min at 35°C with 5 μM fura-2/AM (Molecular Probes) and imaged with a silicon-intensified target (SIT) or an intensified charge-coupled device (ICCD) camera through a 1.3 numerical aperture ×40 oil fluorescence objective (Nikon) (18). The mean calcium value (Table 1) for a given patient consisted of data obtained from 50–100 cells (from 14 control, 5 MELAS, and 4 K–S patients).

Mitochondrial Imaging. Fibroblast mitochondria were labeled with 500 nM 5,5′,6,6′-tetrachloro-1,1′,3,3′-tetraethylbenzimidazolocarbocyanine (JC-1, Molecular Probes) (19, 20). Images were obtained at an excitation wavelength of 488 nm with a confocal laser-scanning microscope (Noran Odyssey with a Nikon Diaphot and a 5-mW argon laser) equipped with two photomultiplier tubes (PMTs). The optical train consisted of a 1.4 numerical aperture ×60 oil objective, a 515-nm long pass barrier filter, a 50-μm confocal slit, and a 560-nm beam-splitting dichroic mirror that directed wavelengths >560 nm to PMT-1 (590 nm, emission) and <560 nm to PMT-2 (527 nm, emission). Secondary 565- to 615-nm and 520- to 560-nm band pass barrier filters were placed before PMT-1 and PMT-2, respectively, to reduce cross-contamination of emission light. Images were acquired from randomly selected fields of nonconfluent cells. Background images were obtained from a cell-free section of the coverslip. A ratio image was generated by dividing the 590-nm image by the 527-nm image (see Fig. 3). Control and MELAS fibroblasts have indistinguishable 527-nm emissions, indicating that MELAS mitochondria maintain sufficient polarization to load JC-1 (see Fig. 3*B*). A mask of the 527-nm emission was applied to the ratio image to eliminate nonmitochondrial features (see Fig. 3). While our method does not give a mitochondrial potential, it offers the powerful advantage of normalization provided by ratiometric techniques. Loew *et al.* (21) have described *in situ* measurement of mitochondrial potential, but their method is unsuitable for our preparation.

Cell Potential Recordings. Membrane potential was measured with 4 M KCl-filled microelectrodes (30–40 MΩ).

RESULTS

MELAS fibroblasts had significantly elevated baseline Ca_i^{2+}, compared to control (Table 1 and Figs. 1 and 2). Ca_i^{2+} levels in controls were identical to values from other laboratories (22, 23). K–S fibroblasts provided another control for baseline Ca_i^{2+} (2–4, 6, 15). Despite the severity of this disease, K–S fibroblasts express very few mtDNA deletions *in vitro*, and Ca_i^{2+} levels were not elevated (Table 1 and Fig. 2*A*). Regression analysis of all evaluable patients showed no correlation between age or sex and baseline Ca_i^{2+} measurements ($P = 0.79$ and 0.40, for age and sex, respectively; *t* test). The mitochondrial inhibitor 3-nitropropionic acid (1 mM) elevated baseline Ca_i^{2+} in control cultures from 79.2 ± 2.6 to 108.3 ± 5.8 nM ($P < 0.001$), resembling baseline Ca_i^{2+} observed in MELAS fibroblasts. Interestingly, 3-nitropropionic acid (1 mM, 18 h) was not toxic to either MELAS or control fibroblasts (<0.02% cell death by trypan blue).

When depolarized with 60 mM potassium, Ca_i^{2+} in control cells increased transiently and then returned to baseline within 3–5 min, even in the continued presence of elevated K^+ (Figs. 1*A* and 2*B*). Identical treatment of MELAS fibroblasts caused sustained elevations in Ca_i^{2+} levels (Figs. 1*B* and 2). Eighty-two of the 520 MELAS fibroblasts examined maintained Ca_i^{2+} at >2 SD above baseline after a 20-min exposure to elevated

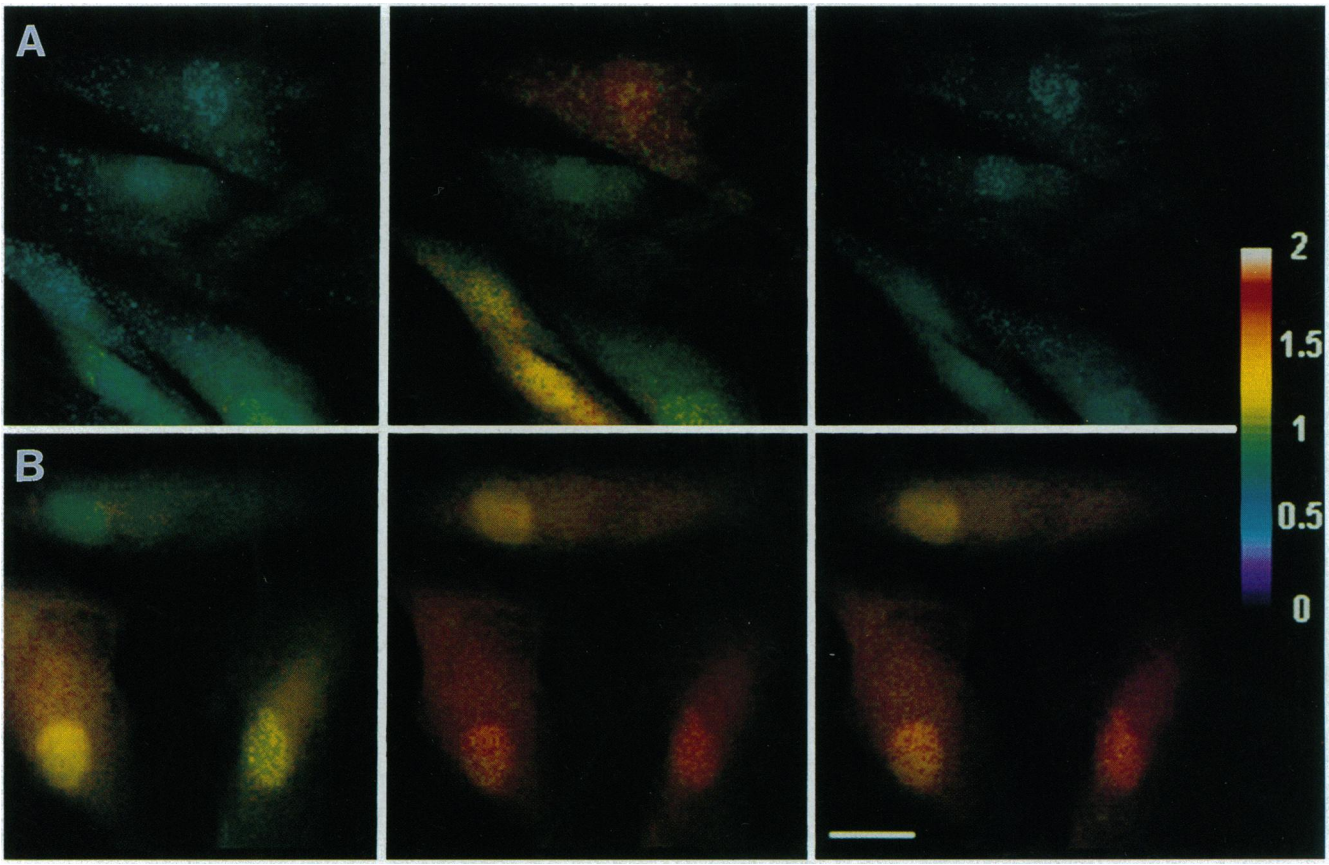

FIG. 1. Fura-2 ratio images of fibroblast Ca_i^{2+} during potassium-induced depolarization. Images are of control (*A*) and MELAS (*B*) fibroblasts, showing baseline Ca_i^{2+} (*Left*) and Ca_i^{2+} after ≈2 (*Center*) and 13 (*Right*) min of continuous depolarization with 60 mM potassium. Color scale indicates 340/380-nm ratio value. (Bar = 10 μm.)

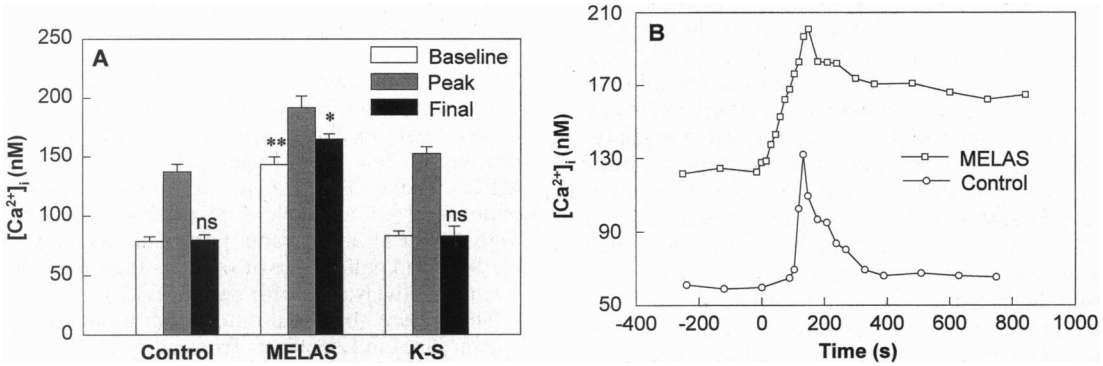

FIG. 2. Altered calcium homeostasis in MELAS fibroblasts. (*A*) Baseline Ca_i^{2+} in MELAS fibroblasts ($n = 5$) is significantly elevated above levels in controls ($n = 14$). K–S fibroblasts ($n = 4$) have baseline Ca_i^{2+} indistinguishable from controls. The final Ca_i^{2+} level was elevated only in MELAS fibroblasts. Bars represent the mean ± SEM. ns, Not significant; *, $P < 0.05$; **, $P < 0.01$ vs. controls by Mann–Whitney test. (*B*) Ca_i^{2+} responses to K^+-induced depolarization in individual control and MELAS fibroblasts.

potassium, compared to 0 of 584 control fibroblasts ($P < 0.001$ by χ^2 test). Prolonged exposure (24 h) to elevated potassium did not result in cell death in either control or MELAS fibroblasts (data not shown).

One explanation for elevated Ca_i^{2+} levels in the MELAS fibroblasts was that low ATP levels might impair Ca_i^{2+} extrusion and sequestration. We assayed ATP levels to determine whether mitochondrial impairment decreased ATP concentrations. ATP in controls was 136 ± 56 μmol of ATP per g of total protein ($n = 6$) compared to 152 ± 46 in MELAS ($n = 3$) (not significant, $P > 0.6$). Both these values are close to other reports for human fibroblasts (24–26).

By using intracellular recording, the resting potential of control fibroblasts was −49.2 ± 4.8 mV ($n = 23$) compared to −48.1 ± 3.8 mV ($n = 19$) for the MELAS fibroblasts ($P > 0.4$), making it unlikely that voltage-sensitive calcium channels, and therefore calcium entry, are different between control and MELAS cells at rest. In addition, the magnitude of calcium elevation after depolarization was similar in both control and MELAS cells (Fig. 2*B*), even though the resting calcium levels in MELAS fibroblasts were elevated above control baseline. This suggests that calcium influx through voltage-sensitive calcium channels was not different in control and MELAS fibroblasts.

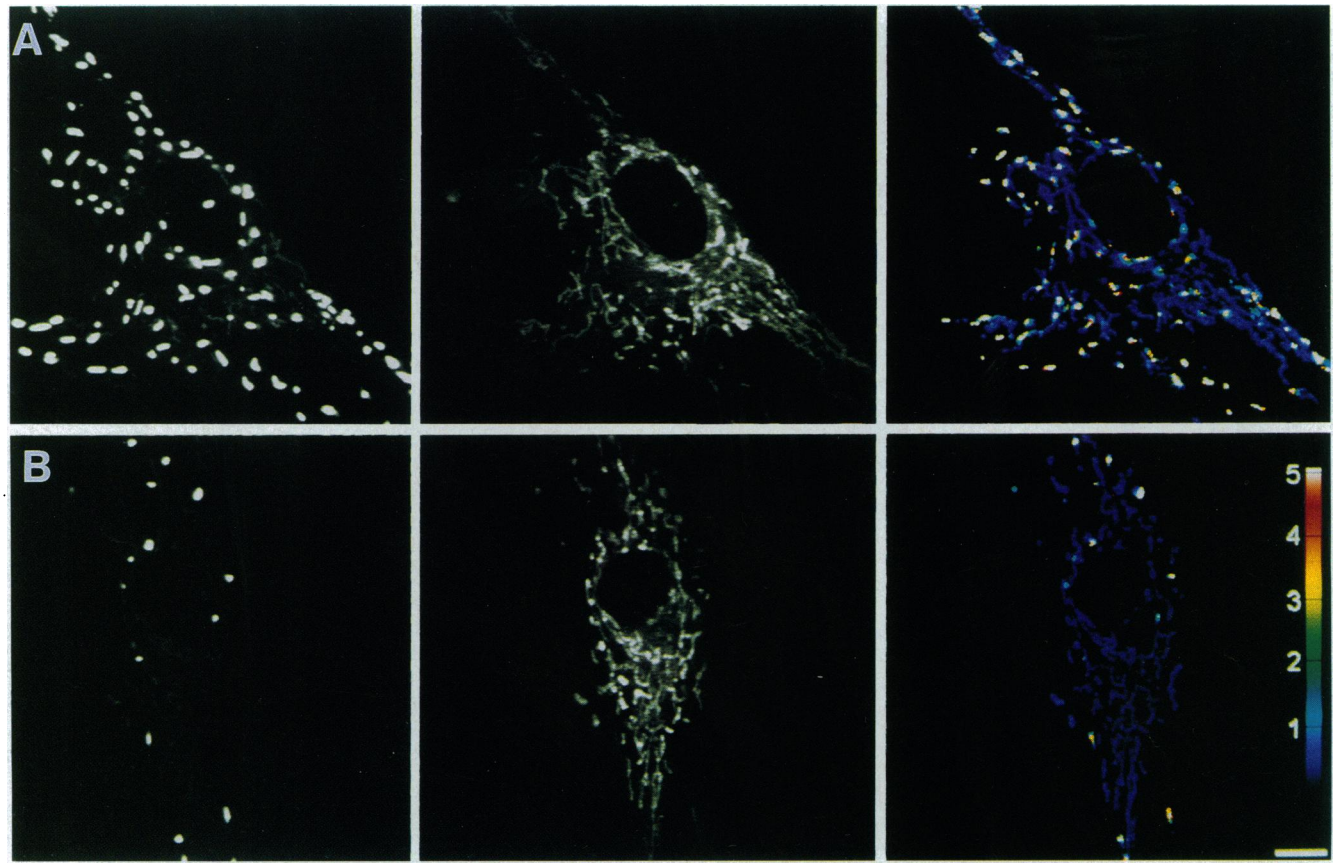

FIG. 3. Confocal micrographs of mitochondria in fibroblasts from control and MELAS patients, visualized with the ratiometric dye JC-1. Representative age- and sex-matched control (*A*) and MELAS (*B*) fibroblasts are shown. (*Left*) Potential-sensitive 590-nm emission. (*Center*) The 527-nm emission. (*Right*) Ratio of the 590/527-nm image. A binary mask of the 527-nm image was applied to the ratio to eliminate all nonmitochondrial features. Color scale indicates 590/527-nm ratio value. (Bar = 10 μm.)

An abnormally low mitochondrial membrane potential (normally, −180 mV) could diminish Ca_i^{2+} uptake through the mitochondrial calcium uniport and impair Ca_i^{2+} sequestration by MELAS mitochondria. Therefore, we measured membrane potential of individual mitochondria in intact fibroblasts by using confocal microscopy and the dual emission dye JC-1 (19, 20). JC-1 selectively labels mitochondria and reports mitochondrial membrane potential as a function of dye aggregation state. JC-1 is maximally excited at 490 nm and emits at 527 and 590 nm. The fluorescence intensity of the 527-nm emission is insensitive to changes in mitochondrial potential, whereas the 590-nm emission linearly increases as a function of mitochondrial potential, due to micellar dye aggregation (Fig. 3 *Left* and *Center*) (19). Other investigators have used the dye as a measure of mitochondrial potential in flow cytometry experiments (27). We have developed a semiquantitative measurement of mitochondrial membrane potential *in situ* by using the ratio of 590/527-nm emission (Fig. 3 *Right*) and confirmed that several mitochondrial inhibitors or uncouplers (1 μM rotenone, 1 μM antimycin, or 1 μM carbonylcyanide *p*-trifluoromethoxyphenylhydrazone) reduce the JC-1 ratio in control fibroblasts (data not shown).

Mitochondrial membrane potentials were compared by using JC-1 ratio imaging. The entire data set (>5 × 10^6 pixels) of 590/527-nm ratio values from control and MELAS mitochondria revealed a distribution clearly skewed toward higher ratios in controls (Fig. 4). Ratio values ≥1 were quantitated to provide a measure of regions with J-aggregate formation, indicating "energized" mitochondria. By using this arbitrary division, ≈22% of control mitochondria, as a population, are "energized," whereas only 11% of MELAS mitochondria are similarly energized (Fig. 4, see dotted lines). When the data were analyzed by patient, ≈20% of the mitochondrial area of control fibroblasts was energized, but <10% of the area of MELAS mitochondria was similarly energized (Table 1 and Fig. 4 *Inset*). Although the initial definition of ratio values ≥1 is an arbitrary division of quiescent and energized mitochondrial membrane potential, the final histogram distribution reveals that for every ratio value ≥0.5, the representation of control mitochondria exceeds that of MELAS mitochondria (Fig. 4).

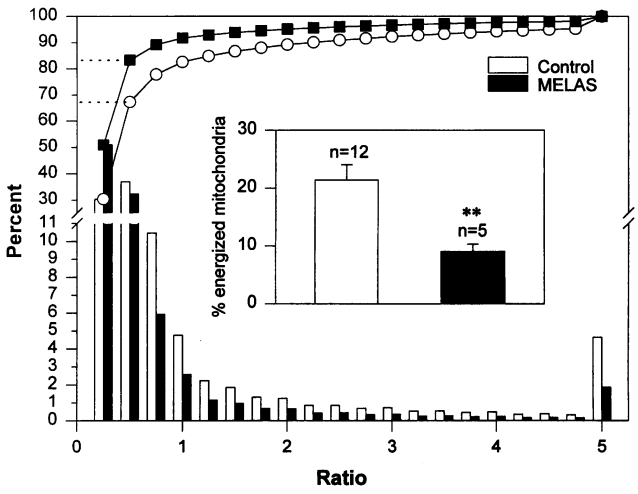

FIG. 4. Analysis of mitochondrial membrane potential in MELAS and control fibroblasts stained with JC-1. Histogram of the entire data set is skewed toward a lower ratio for the MELAS mitochondria. The cumulative total is plotted above each bin for both data sets. When an arbitrary ratio value of 1 is used to distinguish quiescent (<1) and energized (≥1) mitochondria, >89% of MELAS mitochondria, as a population, are quiescent, compared to 78% of control mitochondria (see dotted lines). (*Inset*) An alternative method of analysis uses the same data set but segregates the data by individual patient instead of pooling all pixels (see Table 1). When the two groups are compared in this way, the percent energized mitochondria (ratio ≥1) is still twice as high in the control group. Bars represent the mean ± SEM and *n* is the number of patients. **, $P = 0.002$ by Mann–Whitney test.

Qualitative examination of the JC-1 images is consistent with these observations. There are many J-aggregates with intense 590-nm fluorescence in mitochondria from control fibroblasts, but such J-aggregates are nearly absent from MELAS cells (Fig. 3 *Left*). Regression analysis of control patients listed in Table 1 showed no correlation between mitochondrial membrane potential, as measured by this method, and patient age or sex ($P = 0.24$ and 0.40, for age and sex, respectively; *t* test for variances).

There were abnormal mitochondria (swollen and spherical appearance) in fibroblasts from all five MELAS patients (88 of 223 fields, 1–3 cells per field). Very few morphological abnormalities were present in fibroblasts from 12 control patients (12 of 310 image fields; $P < 0.0001$ by χ^2). This observation confirms findings of other laboratories (28, 29). Interestingly, these abnormal mitochondria always had low JC-1 ratio values (<1).

DISCUSSION

Fibroblasts cultured from patients with MELAS demonstrated sustained abnormalities of calcium homeostasis and mitochondrial membrane potential. While the experimental manipulations employed in this study to increase cytosolic calcium were not toxic to either control or MELAS fibroblasts, we postulate that even modest Ca_i^{2+} elevation, persisting over months or years, could lead to cell injury or death. The cells most vulnerable to calcium-dependent injury would be those that are electrically active, the neurons and muscle cells that experience large calcium influxes during synaptically mediated depolarizations. These are the cells most often affected in MELAS patients (2–6, 10–15). Additionally, mitochondrial compromise may sensitize vulnerable cells to other insults, such as glutamate-induced neurotoxicity. This may account for the neuroprotective effects of glutamate antagonists in some animal models in which mitochondrial toxins produce selective striatal injury (30–33). Dykens (34) recently proposed increased free radical production by mitochondria in the presence of exogenous calcium. Elevated Ca_i^{2+} levels, if present in the muscle and neuronal cells of MELAS patients, may exacerbate oxidative injury and contribute to the manifestation of mitochondrial encephalomyopathy.

There was some variability in baseline values and in Ca_i^{2+} responses to depolarization. The sustained Ca_i^{2+} increases were not seen uniformly in all cells from cultures with mitochondrial defects, presumably due to the heteroplasmic nature of mtDNA (2). Additionally, a threshold, possibly exceeding 90% of mutant mtDNA, may be required for the development of clinical symptoms (35). The observed Ca_i^{2+} variations may be the cellular concomitant of these effects.

JC-1 reveals heterogeneities in mitochondrial membrane potential, results that confirm observations by Smiley *et al.* (20). Although the underlying biophysical basis of J-aggregate formation is not fully understood, we find significantly reduced amounts of J-aggregates in MELAS fibroblasts (Figs. 3 and 4). In addition, we have observed abnormal mitochondrial morphology in MELAS fibroblasts, confirming previous studies (28, 29). The most commonly observed abnormality was swollen spherical mitochondria with low (<1) JC-1 ratio values. This may be indicative of individual mitochondria containing high amounts of mutant mtDNA, which in turn correspond to relatively depolarized transmembrane potentials. The observed reduction of J-aggregates in the MELAS fibroblasts may indicate a decreased electrochemical gradient for Ca_i^{2+} across the mitochondrial membrane resulting in diminished calcium buffering by the mitochondrion in these cells. There is already experimental verification that mitochon-

dria contribute to cytosolic calcium homeostasis in many cell types (36–39).

Our observations do not precisely show how the primary genetic defect in MELAS translates into abnormal mitochondrial polarization. A reasonable hypothesis is that the tRNA mutation results in functionally defective mitochondria that are unable to sustain normal mitochondrial membrane resting potential. In any case, these results provide clear documentation of an abnormality of Ca_i^{2+} homeostasis in a human encephalomyopathy and may have relevance to an "impaired energy" hypothesis (1, 30–33) in human neurodegenerative diseases.

We thank Nancy Lancaster for help in culture preparation and Drs. Michael Watson and Bruce Dowton for identifying and retrieving control and disease fibroblast cultures from storage. Drs. Laura Dugan, Eugene Johnson, Jeff Lichtman, and Eric Schon provided helpful critiques of this work. The research was supported by National Institutes of Health Grants NS-199888 (S.M.R.), NS-01543 (M.P.G.), NS-32140 (M.P.G.), and 5T32NS07057 (S.D.H.) and the Colleen Giblin Charitable Foundation for Pediatric Neurology Research (D.C.D.).

1. Coyle, J. T. & Puttfarcken, P. (1993) *Science* **262,** 689–695.
2. DiMauro, S. & Moraes, C. T. (1993) *Arch. Neurol.* **50,** 1197–1208.
3. Harding, A. E. (1991) *Trends Neurosci.* **14,** 132–138.
4. Karpati, G., Arnold, P., Matthews, P., Carpenter, S., Andermann, F. & Shoubridge, E. (1991) *Rev. Neurol.* **147,** 455–461.
5. Tritschler, H.-J. & Medori, R. (1993) *Neurology* **43,** 280–288.
6. Wallace, D. C. (1992) *Science* **256,** 628–632.
7. Schanne, F. A. X., Kane, A. B., Young, E. E. & Farber, J. L. (1979) *Science* **206,** 700–702.
8. Farber, J. L., Chien, K. R. & Mittnacht, S., Jr. (1981) *Am. J. Pathol.* **102,** 271–281.
9. Simon, R. P., Griffiths, T., Evans, M. C., Swan, J. H. & Meldrum, B. S. (1984) *J. Cereb. Blood Flow Metab.* **4,** 350–361.
10. Ciafaloni, E., Ricci, E., Shanske, S., Moraes, C. T., Silvestri, G., Hirano, M., Simonetti, S., Angelini, C., Donati, M. A., Garcia, C., Martinuzzi, A., Mosewich, R., Servidei, S., Zammarchi, E., Bonilla, E., DeVivo, D. C., Rowland, L. P., Schon, E. A. & DiMauro, S. (1992) *Ann. Neurol.* **31,** 391–398.
11. Pavlakis, S. G., Phillips, P. C., DiMauro, S., DeVivo, D. C. & Rowland, L. P. (1984) *Ann. Neurol.* **16,** 481–488.
12. Goto, Y., Nonaka, I. & Horai, S. (1990) *Nature (London)* **348,** 651–653.
13. Goto, Y., Nonaka, I. & Horai, S. (1991) *Biochim. Biophys. Acta* **1097,** 238–240.
14. Goto, Y., Horai, S., Matsuoka, T., Koga, Y., Nihei, K., Kobayashi, M. & Nonaka, I. (1992) *Neurology* **42,** 545–550.
15. Moraes, C. T., DiMauro, S., Zeviani, M., Lombes, A., Shanske, S., Miranda, A. F., Nakase, H., Bonilla, E., Werneck, L. C., Servidei, S., Nonaka, I., Koga, Y., Spiro, A. J., Brownell, A. K. W., Schmidt, B., Schotland, D. L., Zupanc, M., DeVivo, D. C., Schon, E. A. & Rowland, L. P. (1989) *N. Engl. J. Med.* **320,** 1293–1299.
16. Lowry, O. H. & Passoneau, J. V. (1972) *A Flexible System of Enzymatic Analysis* (Academic, New York), pp. 151–156.
17. Lowry, O. H., Rosebrough, N. J., Farr, A. L. & Randell, R. J. (1951) *J. Biol. Chem.* **193,** 265–275.
18. Moudy, A. M., Yamada, K. A. & Rothman, S. M. (1994) *Neuropharmacology* **33,** 953–962.
19. Reers, M., Smith, T. W. & Chen, L. B. (1991) *Biochemistry* **30,** 4480–4486.
20. Smiley, S. T., Reers, M., Mottola-Hartshorn, C., Lin, M., Chen, A., Smith, T. W., Steele, G. D., Jr., & Chen, L. B. (1991) *Proc. Natl. Acad. Sci. USA* **88,** 3671–3675.
21. Loew, L. M., Tuft, R. A., Carrington, W. & Fay, F. S. (1993) *Biophys. J.* **65,** 2396–2407.
22. Etcheberrigaray, R., Ito, E., Kim, S. & Alkon, D. L. (1994) *Science* **264,** 276–279.
23. Etcheberrigaray, R., Ito, E., Oka, K., Tofel-Grehl, B., Gibson, G. E. & Alkon, D. L. (1993) *Proc. Natl. Acad. Sci. USA* **90,** 8209–8213.
24. Fox, I. H., Shefner, R., Palmieri, G. M. & Bertorini, T. E. (1985) *Neurology* **35,** 1521–1524.
25. Muggleton-Harris, A. L. & Defuria, R. (1985) *In Vitro Cell. Dev. Biol.* **21,** 271–276.
26. Gronostajski, R. M., Pardee, A. B. & Goldberg, A. L. (1985) *J. Biol. Chem.* **260,** 3344–3349.
27. Cossarizza, A., Baccarani-Contri, M., Kalashnikova, G. & Franceschi, C. (1993) *Biochem. Biophys. Res. Commun.* **197,** 40–45.
28. Agsteribbe, E., Huckriede, A., Veenhuis, M., Ruiters, M. H. J., Niezen-Koning, K. E., Skjeldal, O. H., Skullerud, K., Gupta, R. S., Hallberg, R., van Diggelen, O. P. & Scholte, H. R. (1993) *Biochem. Biophys. Res. Commun.* **193,** 146–154.
29. Herzberg, N. H., Middelkoop, E., Adorf, M., Dekkar, H. L., van Galen, M. J. M., van den Berg, M., Bolhuis, P. A. & van den Bogert, C. (1993) *Eur. J. Cell Biol.* **61,** 400–408.
30. Beal, M. F. (1992) *Ann. Neurol.* **31,** 119–130.
31. Beal, M. F., Hyman, B. T. & Koroshetz, W. (1993) *Trends Neurosci.* **16,** 125–131.
32. Albin, R. L. & Greenamyre, J. T. (1992) *Neurology* **42,** 733–738.
33. Turski, L. & Turski, W. A. (1993) *Experientia* **49,** 1064–1072.
34. Dykens, J. A. (1994) *J. Neurochem.* **63,** 584–591.
35. Moraes, C. T., Ciacci, F., Bonilla, E., Jensen, C., Hirano, M., Rao, N., Lovelance, R. E., Rowland, L. P., Schon, E. A. & DiMauro, S. (1993) *J. Clin. Invest.* **92,** 2906–2915.
36. Werth, J. L. & Thayer, S. A. (1994) *J. Neurosci.* **14,** 348–356.
37. Connor, J. A. (1993) *Cell Calcium* **14,** 185–200.
38. Carafoli, E. (1987) *Annu. Rev. Biochem.* **56,** 395–433.
39. Nicholls, D. G. (1985) *Prog. Brain Res.* **63,** 97–106.